Algebra and Condensed Matter

R. Matthias Geilhufe
(Nordita, Stockholm University, KTH - Royal Institute of Technology)

matthias.geilhufe@su.se

Introduction

Condensed matter physics deals with the properties of matter at low temperatures. It aims to describe the microscopic origin of macroscopic phenomena. The macroscopic properties are strongly bound to the phase of matter, for example: solid, characterized by structural rigidity; ferromagnet, characterized by a finite magnetization; superconductor, characterized by a vanishing electrical resistivity. A phase transition denotes the sudden change of a macroscopic property depending on a control parameter, e.g., temperature, pressure, chemical composition.

The difficulty of the subject lies in the complexity of the many-body problem. For example, 1 cm^3 iron contains $\approx 8.5 \times 10^{22}$ iron atoms with $\approx 2.2 \times 10^{24}$ electrons in total. At the same time, the complexity leads to an incredible richness of physical phenomena.

Among others, algebraic methods help in the classification of states of matter, the formulation of effective theories, or determining degenerate levels in spectra. The aim of the present paper is to introduce these ideas to a broad audience of mathematics background. We will focus on a few key examples.

We start with a brief outline of the mathematical framework of quantum mechanics. Next, we show how symmetries in quantum mechanical systems determine level degeneracies. We motivate this result with two examples, first discussing an atomic system and second a crystal, i.e., a lattice-periodic solid. Afterwards, we show how symmetries can be used to formulate an effective theory for electronic states in materials. Such effective theories are often sufficient to study the low temperature properties of complex materials. At the final part of this survey, we introduce the phenomenological theory of phase transitions. Here, again, symmetry is a key ingredient.

By no means does this review cover the full spectrum of relevant topics in condensed matter theory nor the potential computer algebra has in the field. Already, the few examples picked are only tiny bits of entire fields of study. Often, I do not provide a fair account of relevant references. Whenever possible I refer to a review article which might guide the interested reader.

Quantum mechanics

Phenomena of submicroscopic particles are governed by quantum mechanics. Its development about 100 years ago counts as one of the most significant breakthroughs in physics history. In quantum mechanics, a system is described by a state vector $|\psi\rangle \in \mathcal{H}$ in a Hilbert space $\mathcal{H}$. Typically, $\mathcal{H}$ is defined over the field of the complex numbers $\mathbb{C}$. We use the so-called Dirac or bra-ket-notation. Following the Riesz–Fréchet representation theorem, each vector $|\psi\rangle$ is associated a dual vector $\langle\psi|$. $\langle\psi|$ is a linear functional constituting a map $\mathcal{H} \to \mathbb{C}$. Or, in simple notation, we write the inner product as the *braket* $\langle\psi|\psi\rangle$, which motivates the terms bra-vector $\langle\psi|$ and ket vector $|\psi\rangle$.

Observables, such as momentum or angular momentum are represented by linear operators $\mathrm{O} : \mathcal{H} \to \mathcal{H}$. Traditionally, the operator is chosen to be Hermitian to ensure a real valued spectrum as measured in experiments. However, this restriction has been lifted, e.g., by the development of the PT-symmetric quantum mechanics by Bender and Boetcher [1] (P is the parity operation mapping the position vector $\boldsymbol{r} \to -\boldsymbol{r}$; T is the time-reversal $t \to -t$) or in the so-called non-Hermitian quantum mechanics [2] describing open quantum systems. In the latter, non-Hermitian components represent e.g. source and drain terms.

The dynamics of a quantum system is governed by the Schrödinger equation

$$\mathrm{H}\,|\psi\rangle = \mathrm{i}\hbar\frac{\partial}{\partial t}\,|\psi\rangle\,. \tag{1}$$

Here, H is an energy-valued operator called Hamilton operator. We choose H to be Hermitian. The time is denoted by t and $\hbar$ is the Planck constant. In the case of a static system, i.e., with no explicit time dependence, the Schrödinger equation becomes an eigenvalue equation

$$\mathrm{H}\,|\psi\rangle = E\,|\psi\rangle\,, \tag{2}$$

(a)

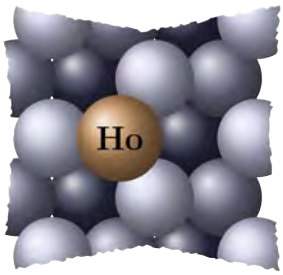

(b)

	Ee	$2\,C_{3z}^{-1}$	$3\,IC_{2D}$
A_1	1	1	1
A_2	1	1	-1
E	2	-1	0

C_1 = {Ee}

$C_2 = \left\{C_{3z}^{-1}, C_{3z}\right\}$

$C_3 = \left\{IC_{2D}, IC_{2C}, IC_{2y}\right\}$

(c)

E (meV)	$\langle J_z \rangle$	Γ
0.	7.9999	E^1
0.	-7.9999	
7.7066	7.0000	E^2
7.7066	-7.0000	
16.3256	0.	A_2^1
16.3259	0.	A_1^1
24.5807	4.9988	E^3
24.5807	-4.9988	
31.7344	3.9967	E^4
31.7344	-3.9967	
37.3103	0.	A_1^2
37.5407	0.	A_2^2
41.5094	1.9952	E^5
41.5094	-1.9952	
43.9529	0.9973	E^6
43.9529	-0.9973	
44.7653	0.	A_1^3

(d)

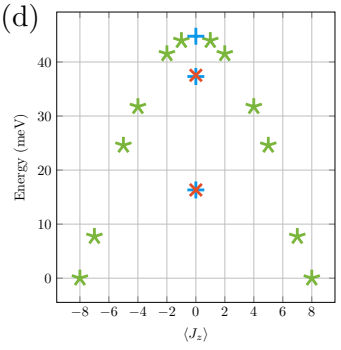

Figure 1: *A Holmium atom on a platinum surface experiences a trigonal potential from the surrounding Pt atoms. As a consequence, the lowest lying Ho state splits with eigenvalues in agreement with the irreducible representations of the group C_{3v}. (a) surface structure. (b) character table of C_{3v}, calculated with GTPack [3, 4]. (c) calculated energy levels. (d) energy levels versus expectation value of the total angular momentum. More details can be found in Ref. [5].*

with E being the energy eigenstate of $|\psi\rangle$. A symmetry U of the Hamiltonian H corresponds to a similarity transformation of H mediated by an invertible operator U,

$$\mathrm{UHU}^{-1} = \mathrm{H}. \tag{3}$$

The set of all symmetries forms a group $\mathcal{G}$. The identity is given by $U = 1$. From equation (3), it follows if $U \in \mathcal{G}$ also $U^{-1} \in \mathcal{G}$. Furthermore, for $U, V \in \mathcal{G}$ it follows from direct computation $UV \in \mathcal{G}$. Applying U from the left to the Schrödinger equation (2) and inserting $1 = \mathrm{U}^{-1}\mathrm{U}$, gives

$$\mathrm{UHU}^{-1}\mathrm{U}\,|\psi\rangle = \mathrm{HU}\,|\psi\rangle = E\mathrm{U}\,|\psi\rangle\,. \tag{4}$$

Hence, if $|\psi\rangle$ is an eigenfunction of H, then also $\mathrm{U}\,|\psi\rangle$ is an eigenfunction. Assuming $\mathcal{G}$ to be a finite group and applying all $U \in \mathcal{G}$ to $|\psi\rangle$, we can project at most d linearly independent vectors $|\psi_1\rangle, \ldots, |\psi_d\rangle$. The matrices given by

$$\mathrm{U}_{ij} = \langle\psi_i|\,\mathrm{U}\,|\psi_j\rangle\,, \tag{5}$$

form an irreducible representation of $\mathcal{G}$. As a consequence, the degeneracy of the energy levels in a quantum system are tightly bound to the dimensions of the irreducible representations of the underlying symmetry group.

Example: degenerate levels

Group theory allows for estimating expected level degeneracy in spectra. This can be of great importance for functionalizing materials by symmetry breaking, e.g., by applying pressure. It also plays a significant role in quantum chemistry. In Figure 1, we show an example for the ground state level splitting of a single Ho atom on a highly conducting Pt surface. Here, the huge magnetic moment of Ho can be switched between two possible states, with measured lifetimes in the order of minutes [5]. On the (111) surface of a Pt crystal, a single Ho atom experiences a trigonal potential from the surrounding Pt atoms. While the ground state of Ho is a high spin state with total angular momentum $J = 8$ for the free atom with spherical symmetry, this state splits into the irreducible representations of C_{3v}, the symmetry group on the surface. C_{3v} is the symmetry group composed of 3-fold rotations about the Cartesian z-axis, and three vertical mirror planes. The group has six elements and three irreducible representations, denoted by A_1 (trivial representation), A_2, and E. According to the Mulliken notation [4], A_1 and A_2 are 1-dimensional and E a 2-dimensional representation. The splitting of the 17-dimensional reducible representation of the $J = 8$ state D^8 is given by

$$D^8 \sim 3A_1 \oplus 2A_2 \oplus 6E. \tag{6}$$

The corresponding numerical values for the Ho energy levels on the surface are given in Figure 1 (c) and (d).

Band structures

Crystals are periodic structures with a lattice spanned by the vectors $\boldsymbol{a}_1, \boldsymbol{a}_2, \boldsymbol{a}_3$. The possible symmetry groups of 3-dimensional (nonmagnetic) crystals are the 230 crystallographic space groups [7]. The irreducible representations of space groups can be denoted by a combined index including the pseudo-momentum $\boldsymbol{k}$ and an additional index running over inequivalent irreducible representations at $\boldsymbol{k}$.

Degenerate levels in band structures can emerge due to two mechanisms [8, 6]:

- **Degenerate levels protected by symmetry.** These are d-fold degenerate levels belonging to a d-dimensional irreducible representation.
- **Degenerate levels protected by band connectivity.** These are $p + q$-fold degenerate *accidental crossings* belonging to two inequivalent irreducible representations of dimensions p and q. They are enforced to occur due to continuous $\boldsymbol{k}$-dependence of the bands and the compatibility relations.

An example for the two kinds of crossings is shown in Figure 2. The band structure corresponds to an organic molecular crystal in space group #19. Here a four-fold

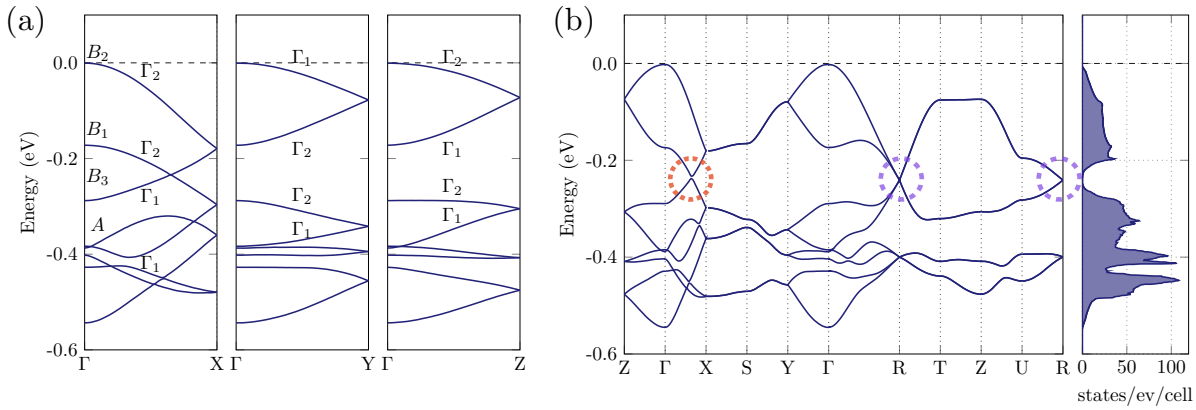

Figure 2: *Electronic band structure of an organic molecular crystal. In the band structure (b), two different kinds of crossings can be found. Degenerate states due to higher dimensional irreducible representations (protected by symmetry) are highlighted in purple. Degenerate states protected by the connectivity of the bands are highlighted in red. (a) shows the dispersion of the electronic band structure together with the corresponding irreducible representations along three paths in the Brillouin zone. While bands belonging to the same representation anti-cross (i.e., form a gap), representations of different representations cross. Therefore, the crossing protected by the band connectivity can not be removed by swapping the 4 relevant electronic states at* Γ *(*A, B_1, B_2, B_3*). Plots are taken from Ref. [6].*

degenerate irreducible representation at the R point on the Brillouin zone boundary leads to a double Dirac crossing (Figure 2 (b)). Additionally, a Dirac crossing can be seen at the path $\overline{\Gamma X}$, which is protected by the connectivity of one-fold degenerate bands emerging at Γ and two-fold degenerate bands in X (Figure 2 (a)).

In the past years, the topological properties of band structures have been intensively investigated. Of particular interest are: topological insulators [9], i.e., materials which are insulating in the bulk, but conducting on the surface; Dirac and Weyl semimetals [10, 11], i.e., materials where low-energy excitations behave as massless fully relativistic fermions; line node semimetals [12, 8], i.e., materials where bands cross in a (closed) line at the Fermi level; systems hosting exotic fermionic excitations [13, 14], e.g., due to tripple band crossings; higher order topological materials, exhibiting nontrivial states at crystal edges or corners [15, 16]. Computer algebraic methods can be used to scan through the massive phase space of allowed Hamiltonians in the 230 space groups. The irreducible representations of space groups can be calculated, e.g., using the Bilbao crystallographic server [17] or GTPack [3, 4].

Effective Hamiltonians

Electrons are fermions. They occupy allowed states following the Pauli principle. At zero temperature, all states up to the Fermi level are occupied. Typical band widths in materials are in the order of a few eV. However, 1 meV corresponds to a temperature of 10 K. As a consequence, only a tiny regime of the band structure is of physical relevance at low temperatures. Therefore, it often suffices to describe a material in terms of an effective Hamiltonian. This can be done in two ways: i) one starts with an actual band structure and performs a low energy expansion around a $\boldsymbol{k}$-point of interest; ii) one starts with the symmetry of the material and generates a symmetry constraint Hamiltonian. Computer algebra can be applied for the latter. Codes allowing for generating effective Hamiltonians are e.g. QSYMM [18], GTPack [3, 4].

To outline the method, we consider a two-dimensional surface with C_{3v} symmetry. We take into account two bands belonging to two different spin-channels. In spin space, an $SU(2)$ rotation matrix can be expressed as $e^{\mathrm{i}\frac{\phi}{2}\boldsymbol{\sigma}\cdot\boldsymbol{n}}$, where ϕ is the rotation angle and $\boldsymbol{n}$ the rotation axis. Hence, we obtain

$$\mathrm{C}_{3z} = \begin{pmatrix} e^{\mathrm{i}\frac{\pi}{3}} & 0 \\ 0 & e^{-\mathrm{i}\frac{\pi}{3}} \end{pmatrix} \tag{7}$$

for the counterclockwise three-fold rotation about the z-axis. Spin is an axial vector similar to the angular momentum and therefore is not affected by inversion. Hence, mirror operations in spin space are given by ordinary rotation matrices. For the case of a reflection $M = IC_{2y}$ one obtains

$$\mathrm{M} = \mathrm{C}_{2y} = \mathrm{i}\sigma_y. \tag{8}$$

Furthermore, we assume time-reversal symmetry, with the time-reversal operation $\mathrm{T} = \mathrm{i}\sigma_y\mathrm{K}$. K is the complex conjugation. From the form of the matrices and the corresponding rotations in the 2-dimensional $\boldsymbol{k}$-space, we can summarize the action of the symmetry elements on $\boldsymbol{k}$ and $\boldsymbol{\sigma}$ as,

$$\mathrm{C}_{3z}: k_\pm \to e^{\pm\mathrm{i}\frac{2\pi}{3}} k_\pm; \tag{9}$$

$$\sigma_\pm \to e^{\pm\mathrm{i}\frac{2\pi}{3}} \sigma_\pm; \sigma_z \to \sigma_z \tag{10}$$

$$\mathrm{M}: k_\pm \to -k_\mp; \tag{11}$$

$$\sigma_{x,z} \to -\sigma_{x,z}; \sigma_z \to \sigma_z \tag{12}$$

$$\mathrm{T}: \boldsymbol{k} \to -\boldsymbol{k}; \boldsymbol{\sigma} \to -\boldsymbol{\sigma}. \tag{13}$$

We use the abbreviations $k_\pm = k_x \pm \mathrm{i}k_y$ and $\sigma_\pm = \sigma_x \pm \mathrm{i}\sigma_y$. The Hamiltonian is invariant under all the symmetries of C_{3v} and time-reversal symmetry. A generic

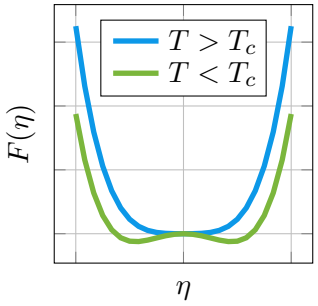

Figure 3: *Phenomenological theory of phase transitions with order parameter η. Below the critical temperature $T < T_c$, the free energy has minima for $\eta \neq 0$. As a result, a system undergoes the transition into an ordered phase. η breaks the symmetry.*

2×2 Hamiltonian can be written as

$$\mathrm{H}(\boldsymbol{k}) = \epsilon(\boldsymbol{k}) + \begin{pmatrix} h(\boldsymbol{k}) & g(\boldsymbol{k}) \\ g^*(\boldsymbol{k}) & -h(\boldsymbol{k}) \end{pmatrix}. \tag{14}$$

We require $h^*(\boldsymbol{k}) = h(\boldsymbol{k})$ for the Hamiltonian to be Hermitian. Furthermore, the symmetry operations constrain the Hamiltonian to satisfy the following conditions,

$$\mathrm{T}\mathrm{H}(\boldsymbol{k})\mathrm{T}^{-1} = \mathrm{H}(-\boldsymbol{k}), \tag{15}$$

$$\mathrm{C}_3\mathrm{H}(k_\pm)\mathrm{C}_3^{-1} = \mathrm{H}(e^{\pm \mathrm{i}\frac{2\pi}{3}} k_\pm), \tag{16}$$

$$\mathrm{M}\mathrm{H}(k_\pm)\mathrm{M}^{-1} = \mathrm{H}(-k_\mp). \tag{17}$$

Time-reversal symmetry leads to $h(-\boldsymbol{k}) = -h(\boldsymbol{k})$ and $g(-\boldsymbol{k}) = -g(\boldsymbol{k})$. The three-fold rotational symmetry gives $h(k_\pm) = h(e^{\mp \mathrm{i}\frac{2\pi}{3}} k_\pm)$ and $e^{\pm \mathrm{i}\frac{2\pi}{3}} g(k_\pm) = g(e^{\mp \mathrm{i}\frac{2\pi}{3}} k_\pm)$, and, last but not least, the mirror symmetry enforces $-h(k_\pm) = h(-k_\mp)$ and $-g^*(k_\pm) = g(-k_\mp)$. To obtain an explicit expression for $h(\boldsymbol{k})$ and $g(\boldsymbol{k})$ we expand both functions in powers of $k_\pm$, $h(\boldsymbol{k}) = a_0 + a_1 k_+ + a_2 k_- + a_3 k_+^2 + \ldots$, and $g(\boldsymbol{k}) = b_0 + b_1 k_+ + b_2 k_- + b_3 k_+^2 + \ldots$. Enforcing the conditions above, we deduce $h(\boldsymbol{k}) = \frac{\lambda}{2}(k_+^3 + k_-^3)$ and $g(\boldsymbol{k}) = -\mathrm{i}k_+$. The resulting low-energy expansion is

$$\mathrm{H}(\boldsymbol{k}) = \epsilon(\boldsymbol{k}) + v_D(\sigma_x k_y - \mathrm{i}\sigma_y k_x) + \frac{\lambda}{2}\left(k_+^3 + k_-^3\right) + \ldots. \tag{18}$$

Here, the first term gives the linear dispersion of the Dirac cone and the corresponding spin-texture. The second term induces hexagonal warping effects. Such hexagonal warping effects can be seen experimentally for the surface states of topological insulators [19].

Phase transitions

According to the Landau-Ginzburg-Wilson theory of phase transitions, a phase is associated to an order parameter introducing a symmetry breaking. For example, the transition into a ferromagnet with finite magnetization breaks time-reversal symmetry. The transition of a normal metal into a superconductor breaks $U(1)$ gauge symmetry. The transition into a ferroelectric material breaks inversion symmetry.

We consider a symmetry group $\mathcal{G}$ with irreducible representations D^p of dimension d_p. The multicomponent order parameter η_i^p, $i = 1, \ldots, d_p$ is a set of basis functions transforming like D^p, i.e., $\forall g \in \mathcal{G} : \mathrm{g}\eta_i = \sum_j D^p_{ji}(g)\,\eta_j$. The free energy F is a scalar function of all present order parameters. F is invariant under all transformations $\mathrm{g} \in \mathcal{G}$ and can be written as a polynomial in the η_i^p.

For example, the simplest case is a scalar order parameter η with the following free energy (see Figure),

$$F(\eta) = a(T - T_c)\eta^2 + b\eta^4, \qquad a, b, > 0. \tag{19}$$

Here, T is the temperature. The phase transition takes place at the critical temperature T_c. In terms of (19), for $T > T_c$ the minimum of the free energy is given for $\eta = 0$. This regime is denoted as the normal phase. Below the critical temperature, $T < T_c$, the free energy has the form of a double well potential with minima at $\eta = \pm\eta_0$. Hence, the system minimizes the free energy by establishing an ordered phase characterized by η.

More complex expressions can be obtained for multicomponent order parameters. For example, a ferroelectric is characterized by a nonzero polarization vector $\boldsymbol{P}$. In a cubic normal phase, the free energy takes the following form up to fourth order

$$F(\boldsymbol{P}) = \alpha_1 \boldsymbol{P}^2 + \alpha_2 \left(P_x P_y + P_x P_z + P_y P_z\right) + \beta\left(P_x^4 + P_y^4 + P_z^4\right). \tag{20}$$

The complexity of expressions for the free energy increases even further by lowering the symmetry of the normal phase or by coupling various order parameters describing different phenomena, e.g., coexistence or competition of ferroelectricity and superconductivity [20].

Computer algebra can be applied to automatically generate expressions for the free energy. Algorithmically, this is achieved by modeling the space of all relevant order parameters by the reducible representation $D = D^{p_1} \oplus D^{p_2} \oplus \ldots$. At each order n, we generate the representation

$$D^{\otimes n} = \underbrace{D \otimes D \otimes \ldots}_{n \text{ times}}. \tag{21}$$

$D^{\otimes n}$ is reducible and can be written in terms of the irreducible representations D^p,

$$D^{\otimes n} \sim n_1 D^1 \oplus n_2 D^2 \oplus \dots . \tag{22}$$

D^1 denotes the identity representation. The free energy F transforms as D^1. Therefore, we need to generate linearly independent terms of the n_1 products of $\eta_j^{p_i}$ which transform as D^1. The n_1 basis functions transforming as D^1 are constructred using Clebsch-Gordan coefficients. The Clebsch-Gordan coefficients mediate the similarity transformation between the reducible representation $D^{\otimes n}$ and it's block diagonal form. Clebsch-Gordan coefficients can be calculated, e.g., using the algorithm of van Den Broek and Cornwell [21].

Intertwined order

Complex materials can exhibit a rich phase diagram with several phase boundaries. By now it has been understood that fluctuations in one phase can mediate the mechanism to stabilize another phase. For example, fluctuations around the quantum critical point to a ferroelectric transition can mediate superconductivity [22]. Furthermore, instead of considering several phases as competing independent states, many cases are known with intertwined order [23, 24]. In such materials, neither of the two phases η_i^p nor η_j^q are present, but instead the composite order $\eta_i^p \eta_j^q$. While η_i^p and η_j^q are basis functions of the irreducible representation D^p and D^q, the composite order parameter $\eta_i^p \eta_j^q$ transforms as the generally reducible representation $D^{p\otimes q} = D^p \otimes D^q$. This representation can be decomposed into the irreducible representations

$$D^{p\otimes q} \sim n_1 D^1 \oplus n_2 D^2 \oplus \dots . \tag{23}$$

Each of the irreducible representations on the right-hand side represent an independent composite order parameter. While the basis functions of the occurring irreducible representations have the same properties as the single phases discussed in the previous section, the observable physical phenomena strongly depend on the composition of the parent phases. Exploring and classifying allowed composite phases in the 230 space groups is a tedious task which can be automatized using the methods of computer algebra.

Conclusion and outlook

The properties of matter are determined from a complex interacting quantum many-body problem. Computer algebra can be applied to formulate effective theories or to classify and discuss allowed solutions. Symmetry is the key ingredient for formulating, e.g., an effective Hamiltonian or free energy expansion.

Several branches of condensed matter physics rely on algebraic methods. For example, with the discovery of topological properties of matter in the 1980s [25, 26, 27] and the experimental realization of topological insulators in the 2000s [28], huge interest has emerged in classifying electronic band structures in 2- and 3-dimensional solids for the past two decades. Recently, this effort was extended, e.g.: i) to dimensions > 3, due to the correspondence of higher dimensional periodic lattices to 2- and 3-dimensional quasiperiodic structures [29]; ii) space- and time-periodic systems, i.e., Floquet-Bloch spectra [30].

Time-dependence also plays a significant role in discovering novel time-dependent or non-equilibrium orders, e.g., time crystals [31, 32], odd-frequency pairing [33], transient superconductivity [34]. The complexity of non-equilibrium phenomena clearly calls for novel algebraic techniques.

References

[1] Carl M Bender and Stefan Boettcher. Real spectra in non-Hermitian Hamiltonians having $\mathcal{PT}$ symmetry. *Physical Review Letters*, 80(24):5243, 1998.

[2] Yuto Ashida, Zongping Gong, and Masahito Ueda. Non-hermitian physics. *Advances in Physics*, 69(3):249–435, 2020.

[3] R. M. Geilhufe and Wolfram Hergert. GTPack: A Mathematica Group Theory Package for Application in Solid-State Physics and Photonics. *Frontiers in Physics*, 6:86, 2018.

[4] Wolfram Hergert and R. M. Geilhufe. *Group Theory in Solid State Physics and Photonics: Problem Solving with Mathematica*. Wiley-VCH, 2018. ISBN: 978-3-527-41133-7.

[5] Toshio Miyamachi, Tobias Schuh, Tobias Märkl, Christopher Bresch, Timofey Balashov, Alexander Stöhr, Christian Karlewski, Stephan André, Michael Marthaler, Martin Hoffmann, et al. Stabilizing the magnetic moment of single holmium atoms by symmetry. *Nature*, 503(7475):242–246, 2013.

[6] R Matthias Geilhufe, Stanislav S Borysov, Adrien Bouhon, and Alexander V Balatsky. Data mining for three-dimensional organic Dirac materials: focus on space group 19. *Scientific reports*, 7(1):1–7, 2017.

[7] Carolyn Pratt Brock, T Hahn, H Wondratschek, U Müller, U Shmueli, E Prince, A Authier, V Kopskỳ, DB Litvin, E Arnold, et al. International tables for crystallography volume A: Space-group symmetry, 2016.

[8] R Matthias Geilhufe, Adrien Bouhon, Stanislav S Borysov, and Alexander V Balatsky. Three-dimensional organic Dirac-line materials due to nonsymmorphic symmetry: A data mining approach. *Physical Review B*, 95(4):041103, 2017.

[9] M Zahid Hasan and Charles L Kane. Colloquium: topological insulators. *Reviews of Modern Physics*, 82(4):3045, 2010.

[10] Tim O Wehling, Annica M Black-Schaffer, and Alexander V Balatsky. Dirac materials. *Advances in Physics*, 63(1):1–76, 2014.

[11] NP Armitage, EJ Mele, and Ashvin Vishwanath. Weyl and Dirac semimetals in three-dimensional solids. *Reviews of Modern Physics*, 90(1):015001, 2018.

[12] A. A. Burkov, M. D. Hook, and Leon Balents. Topological nodal semimetals. *Physical Review B*, 84:235126, Dec 2011.

[13] Barry Bradlyn, Jennifer Cano, Zhijun Wang, MG Vergniory, C Felser, Robert Joseph Cava, and B Andrei Bernevig. Beyond Dirac and Weyl fermions: Unconventional quasiparticles in conventional crystals. *Science*, 353(6299), 2016.

[14] Zhijun Wang, Aris Alexandradinata, Robert J Cava, and B Andrei Bernevig. Hourglass fermions. *Nature*, 532(7598):189–194, 2016.

[15] Flore K Kunst, Guido van Miert, and Emil J Bergholtz. Lattice models with exactly solvable topological hinge and corner states. *Physical Review B*, 97(24):241405, 2018.

[16] Sayed Ali Akbar Ghorashi, Tianhe Li, and Taylor L. Hughes. Higher-Order Weyl Semimetals. *Physical Review Letters*, 125:266804, Dec 2020.

[17] Mois I Aroyo, Asen Kirov, Cesar Capillas, JM Perez-Mato, and Hans Wondratschek. Bilbao crystallographic server. ii. representations of crystallographic point groups and space groups. *Acta Crystallographica Section A: Foundations of Crystallography*, 62(2):115–128, 2006.

[18] Dániel Varjas, Tómas Ö Rosdahl, and Anton R Akhmerov. Qsymm: Algorithmic symmetry finding and symmetric Hamiltonian generation. *New Journal of Physics*, 20(9):093026, 2018.

[19] Zhanybek Alpichshev, J. G. Analytis, J.-H. Chu, I. R. Fisher, Y. L. Chen, Z. X. Shen, A. Fang, and A. Kapitulnik. STM Imaging of Electronic Waves on the Surface of Bi_2Te_3: Topologically Protected Surface States and Hexagonal Warping Effects. *Physical Review Letters*, 104:016401, Jan 2010.

[20] Joseph L. Birman and Meir Weger. Theory of coexistence of superconductivity and ferroelectricity: A dynamical symmetry model. *Physical Reviev B*, 64:174503, Oct 2001.

[21] P. M. van Den Broek and J. F. Cornwell. Clebsch-gordan coefficients of symmetry groups. *physica status solidi (b)*, 90(1):211–224, 1978.

[22] Quantum critical origin of the superconducting dome in SrTiO 3, author=Edge, Jonathan M and Kedem, Yaron and Aschauer, Ulrich and Spaldin, Nicola A and Balatsky, Alexander V. *Physical Review Letters*, 115(24):247002, 2015.

[23] Rafael M Fernandes, Peter P Orth, and Jörg Schmalian. Intertwined vestigial order in quantum materials: Nematicity and beyond. *Annual Review of Condensed Matter Physics*, 10:133–154, 2019.

[24] Eduardo Fradkin, Steven A Kivelson, and John M Tranquada. Colloquium: Theory of intertwined orders in high temperature superconductors. *Reviews of Modern Physics*, 87(2):457, 2015.

[25] K. v. Klitzing, G. Dorda, and M. Pepper. New Method for High-Accuracy Determination of the Fine-Structure Constant Based on Quantized Hall Resistance. *Physical Review Letters*, 45:494–497, Aug 1980.

[26] R. B. Laughlin. Quantized hall conductivity in two dimensions. *Physical Review B*, 23:5632–5633, May 1981.

[27] D. J. Thouless, M. Kohmoto, M. P. Nightingale, and M. den Nijs. Quantized Hall Conductance in a Two-Dimensional Periodic Potential. *Physical Review Letters*, 49:405–408, Aug 1982.

[28] YL Chen, James G Analytis, J-H Chu, ZK Liu, S-K Mo, Xiao-Liang Qi, HJ Zhang, DH Lu, Xi Dai, Zhong Fang, et al. Experimental realization of a three-dimensional topological insulator, Bi_2Te_3. *Science*, 325(5937):178–181, 2009.

[29] Yaacov E Kraus, Yoav Lahini, Zohar Ringel, Mor Verbin, and Oded Zilberberg. Topological states and adiabatic pumping in quasicrystals. *Physical Review Letters*, 109(10):106402, 2012.

[30] Alvaro Gómez-León and Gloria Platero. Floquet-bloch theory and topology in periodically driven lattices. *Physical Review Letters*, 110(20):200403, 2013.

[31] Krzysztof Sacha and Jakub Zakrzewski. Time crystals: a review. *Reports on Progress in Physics*, 81(1):016401, 2017.

[32] Xiao Mi, Matteo Ippoliti, Chris Quintana, Amy Greene, Zijun Chen, Jonathan Gross, Frank Arute, Kunal Arya, Juan Atalaya, Ryan Babbush, et al. Observation of Time-Crystalline Eigenstate Order on a Quantum Processor. *arXiv:2107.13571*, 2021.

[33] Jacob Linder and Alexander V Balatsky. Odd-frequency superconductivity. *Reviews of Modern Physics*, 91(4):045005, 2019.

[34] Daniele Fausti, RI Tobey, Nicky Dean, Stefan Kaiser, A Dienst, Matthias C Hoffmann, S Pyon, T Takayama, H Takagi, and Andrea Cavalleri. Light-induced superconductivity in a stripe-ordered cuprate. *Science*, 331(6014):189–191, 2011.